JOURNAL OF MATERIALS SCIENCE 21 (1986) 3957–3965

Interface strength effects on the compressive–flexural/shear failure mode transition of composites subjected to four-point bending

G. C. SHIH
Delsen Testing Laboratories, Inc., Glendale, California 91201, USA

L. J. EBERT
Department of Metallurgy and Materials Science, Case Western Reserve University, Cleveland, Ohio 44106, USA

Wang's microbuckling model [1] has been extended to oriented fibre composites loaded in four-point bending. The modified model shows that when any internal parameter (e.g. the interface strength) is changed, the resultant change of the interlaminar shear strength and that of the compressive strength are always of the same sense. Additionally, the degree of change of the shear strength is always larger than that of the compressive strength. As a consequence of this conclusion, a four-point bend test piece which normally fails in the flexural compressive mode may fail in the shear mode upon interface degradation. This was rationalized with the aid of the failure-mode transition diagram [2]. This diagram has been used to explain the change in bend failure mode resulting from a change of the external parameters, such as the span-to-thickness ratio, and the fibre fraction. Experiments were conducted to verify such a failure-mode transition behaviour for fibreglass composites of different interface conditions, when the flexural compressive failure mechanism was of the microbuckling type.

Nomenclature

σ_{max}	see Equation 1
σ_0	flexural strength
σ_0^-	longitudinal compressive strength
τ_{max}	see Equation 2
τ_0	shear strength
γ_0	shear strain at failure
λ	half wave length of the fibre wavy pattern
w	a parameter in Equation 8
b	width of specimen
f_0	maximum fibre deflection of the initial fibre wavy pattern
G_{12}	secant shear modulus at failure
h	thickness of specimen
K	$4S/h$ (Fig. 2)
K_r	see Equation 4
L	support span (Fig.1)
m	a constant in Equation 8
P	applied maximum load
S	outward span (Fig. 1)
x_1	co-ordinate along the fibre direction in unidirectional composites
x_2	co-ordinate transverse to the fibre direction in unidirectional composites
Z	see Equations 7, 9 and 11

1. Introduction

The importance of oriented fibre-reinforced composite materials lies in their high specific strength along the fibre direction. In real structures, pure axial loading by any mode occurs rarely, and flexural loading is much more common. Because a test piece in the four-point bending test is subjected only to a constant moment in the load span, four-point bending tests of unidirectional composites with fibres aligned in the maximum stress direction are commonly selected for evaluating the mechanical performance of composites.

In a four-point bending test, a constant moment is developed over the test piece in the load span. The magnitude of the maximum flexural stress at the outmost surface layer in the load span is (all the terms in this paper were defined in the "nomenclature" section)

$$\sigma_{max} = \frac{3PS}{bh^2} \quad (1)$$

Also, there is a linear shear–force distribution along the test piece in the outward span. The shear stress reaches its maximum value at the mid-thickness of the test piece in the outward span close to the two loading heads, Fig. 1. The magnitude of such a maximum shear stress is

$$\tau_{max} = \frac{3P}{4bh} \quad (2)$$

Therefore, in a four-point bending test, there are really

0022–2461/86 $03.00 + .12

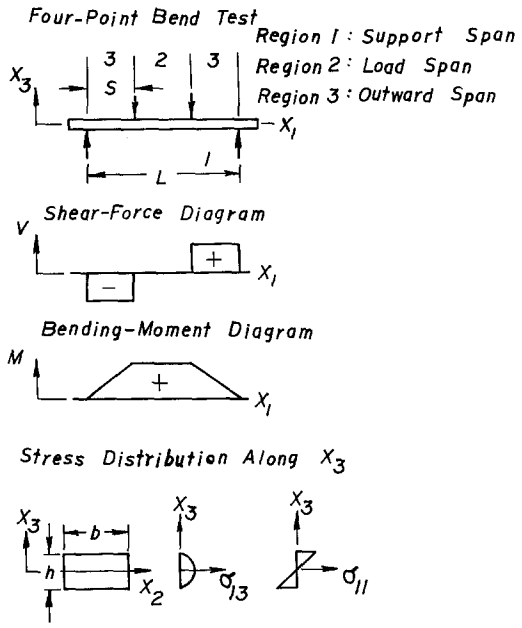

Figure 1 Shear force and bending moment distribution along x_1, and shear stress and flexural stress distribution along x_3 in a four-point bend test.

three potential failure mechanisms – flexural tensile, flexural compressive, and shear – acting at different locations of the test piece and competing with each other. In four-point bending test, while metals having relatively high shear strengths are prone to fail in the flexural mode, composites having shear strength much lower than their flexural strengths tend to fail in the shear mode in the outward span under certain conditions. (Here, flexural strength implies the smaller value between the flexural tensile strength and the flexural compressive strength.) Thus, the failure mode in a four-point bending test may change when any materials/testing parameters are varied. A knowledge of such a failure mode transition behaviour is important since this phenomenon has to be taken into account in the design stage. The purpose of the present study was that of determining, analytically and experimentally, the mode (flexural compressive or shear) by which unidirectional composites will fail in four-point bending when conditions at the fibre/matrix interface are varied. The flexural–tensile failure is discussed elsewhere [3].

2. Background

In a four-point bending test, the maximum shear stress in the test piece reaches the shear strength of the test piece before flexural failure prevails, if the test piece is thick enough. This is best expressed by combining Equations 1 and 2,

$$\sigma_{max} = \frac{4S}{h}\tau_{max} = K\tau_{max} \quad (3)$$

and constructing the failure mode transition diagram [2, 4, 5] accordingly, Fig. 2.

From Equation 3 and Fig. 2, it is seen that when geometries of the fixture and the test-piece satisfy the relation

$$K_r = \left(\frac{4S}{h}\right)_{critical} = \frac{\sigma_0}{\tau_0} \quad (4)$$

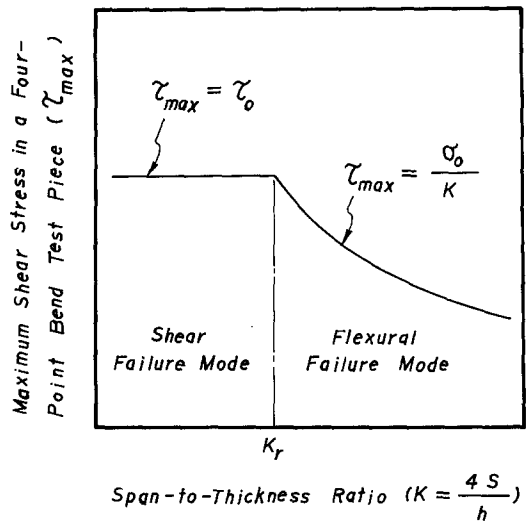

Figure 2 Failure mode transition diagram showing the maximum shear stress in a four-point bend test as a function of span-to-thickness ratio. Note that $K_r = \sigma_0/\tau_0$ at the transition point.

the flexural–shear combined failure mode would result. On the other hand, if $4S/h$ is smaller than σ_0/τ_0, the shear failure mode would occur, and if $4S/h$ is larger than σ_0/τ_0, the flexural failure mode would occur.

Besides the geometries of the fixture and the test piece, internal material properties will also affect such a flexural/shear transition behaviour. Davidovitz *et al.* [6] found that composites with a higher fibre fraction would often introduce a weaker interface, thus resulting in a transition from flexural to shear failure mode. In this study the critical fibre volume fraction was found to be about 45%, and the flexural failure mode was primarily a tensile one. This view point can be made more clear from the failure-mode transition diagram. Since higher fibre fractions (and therefore, weaker interfaces and stronger fibres) lead to composites with a poorer shear strength and a higher tensile strength, the associated failure-mode transition diagram would have an appearance such as the dotted curve shown in Fig. 3. According to Fig. 3, the

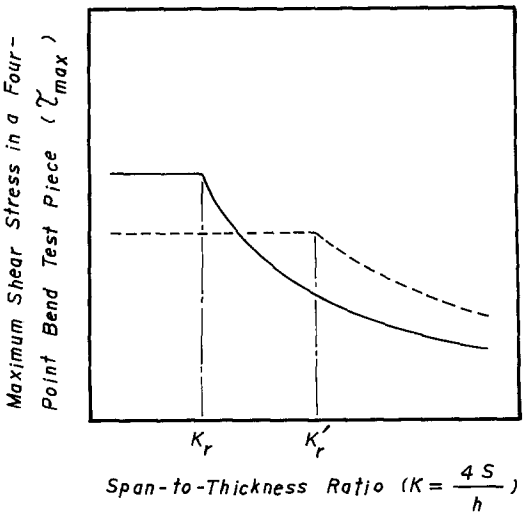

Figure 3 Failure mode transition diagrams for unidirectional composites with different fibre volume fraction. The situation shown is valid only when the fibre/matrix interfacial shear strength is lower than the matrix shear strength. (——) lower fibre fraction; (– – –) higher fibre fraction.

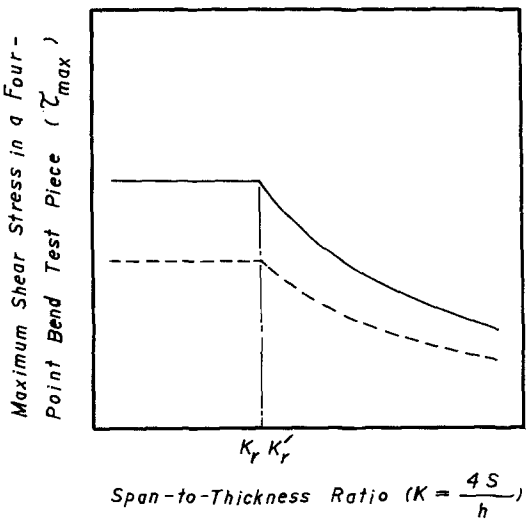

Figure 4 Failure-mode transition diagrams for unidirectional composites with different interface strengths. The situation shown is valid only when the compressive strength and the shear strength are affected by the interface strength to the same extent. (——) higher interface strength; (– – –) lower interface strength.

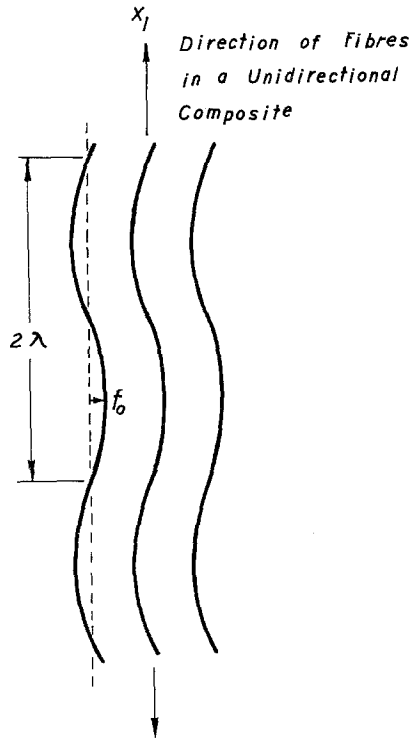

Figure 5 Initial fibre deflection pattern assumed in a stress free unidirectional composite [1].

transition point was shifted to a higher $4S/h$ value as the fibre fraction increased. Because the loading path remained the same throughout Davidovitz's study, the shear failure mode would occur when the fibre fraction exceeded a critical value.

In addition to the geometries of both the fixture and the test piece, and the fibre fraction, the interface strength alone could be another material parameter affecting such failure-mode transition behaviour. When the interface strength is low enough, the composite shear strength would also be low [7–9]. Therefore, the composites would be prone to fail in the shear mode in a four-point bending test, providing that the flexural strength remained essentially the same.

The flexural strength is also affected by the interface conditions to a greater or lesser extent. (While the effect of the interface on the tensile strength was discussed elsewhere [3], this paper will be concentrated on the flexural compressive strength case.) In the flexural compressive failure mode case, the fibre microbuckling mechanism is activated by the breakdown of the fibre/matrix interface. The quantitative dependency of interface strength on the compressive strength is still not quite clear. In cases where both compressive strength and shear strength are reduced by the same percentage as the interface strength decreased, based on Equation 4, the transition point would be essentially the same, as shown in Fig. 4. In real situations, when the interface condition is varied, it is the ratio of the percentage change of the flexural strength to that of the shear strength which determines how the transition point shifts in the failure-mode transition diagram.

On the basis of the above, it is interesting to find the effect of interface condition alone (with fixed fibre fraction) on the flexural (compressive)/shear failure-mode transition behaviour of unidirectional composites subjected to four-point bending tests.

3. Theoretical prediction

3.1. Microbuckling model

Because the microbuckling (local fibre buckling) was found to be the failure mechanism on the compressive side of some failed four-point bending test pieces in the experimental phase of this study, the relation between the interface and the compressive strength will be examined on the basis of the microbuckling mechanism first. A review of the early work of microbuckling can be found in [10]. A concise comment on various models can be found in [1]. A model proposed by Wang [1] took the non-linear shear response of composites and the initial fibre deflection into account, and appeared to be a reasonable one. This model was also adopted and compiled [11] for predicting the longitudinal compressive strength. Therefore, the flexural compressive strength under consideration in this study will be assumed to be the same as the longitudinal compressive strength predicted in this model.

According to Wang [1], fibres in composites had initial deflection even before compression. Such a deflection pattern can be idealized as $f_0 \sin(\pi x_1/\lambda)$ (Fig. 5), and the f_0/λ is in the order of 10^{-2} [1, 12]. Based on values of experimentally determined σ_0^-, it was inferred that [11]

$$\frac{\pi f_0}{\lambda} \geqslant \frac{\tau_0}{G_{12}} \quad \text{for boron/epoxy composites, and} \tag{5}$$

$$\frac{\pi f_0}{\lambda} \geqslant \frac{3\tau_0}{G_{12}} \quad \text{for graphite/epoxy composites}$$

The compressive failure of composites caused by microbuckling of fibres has the compressive strength

value [1]

$$\sigma_0^- = \frac{G_{12}}{1 + \left(\frac{\pi f_0/\lambda}{\tau_0/G_{12}}\right)} \quad (6)$$

The relation between the interface strength and the σ_0^- is not quite apparent in Equation 6. However, because τ_0 is closely related to the interface strength [7–9], the relation between the interface strength and the σ_0^- can readily be found via τ_0. More specifically, when τ_0 varied as a result of change in interface condition, it would be interesting to find the change in the value of σ_0^- according to Equation 6.

3.2. Linear shear response

Harrod and Begley [13] pointed out that the stiffness of composites should not be very sensitive to the nature of the fibre/matrix interface, since the elastic properties are bulk properties and the volume of material in the interphase is relatively small. This viewpoint was later verified from the load–deflection response obtained in the experimental phase of this study. Therefore, G_{12} would be essentially independent of the interface strength when the shear response of the composites is a linear relationship. As a consequence, only σ_0^- and τ_0 were considered as the interface-sensitive parameters in Equation 6. Differentiating Equation 6 yields

$$Z \equiv \frac{d\sigma_0^-/\sigma_0^-}{d\tau_0/\tau_0} = 1 - \frac{\lambda\tau_0}{\lambda\tau_0 + \pi f_0 G_{12}} \quad (7)$$

which provides valuable information. When the interface strength decreases, τ_0 decreases [7–9], and σ_0^- is also reduced, since $d\sigma_0^-/d\tau_0 > 0$. In addition, since $Z < 1$, the percentage change in the compressive strength would be less than that in the shear strength, i.e. the effect of interface strength on τ_0 is greater than that on σ_0^-.

3.3. Non-linear shear response

Normally, the shear response of the composite is non-linear [1, 14] and the tangent shear modulus changes with the shear stress. In this case, direct differentiation on Equation 6 is no longer appropriate.

The development of the effect of the interface strength on the shear stress–strain curve is outside the scope of this study. Nevertheless, one can construct a hypothetical shear stress–strain curve for unidirectional composites, Fig. 6a [1]. As has been discussed in the linear case, the moduli of composites are less affected by the interface conditions [13]. The same conclusion would also hold for the initial tangent moduli of composites in non-linear cases. Therefore, one can further assume that the shear stress–strain curves in different (poorer here for simplicity) interface conditions take the form as shown in Figs 6b and c. By connecting those shear fracture stress–strain points in different interface conditions, one can obtain the shear fracture stress–strain curve, broken lines in Figs 6b, c. These curves can be approximated by

$$\tau_0 = m\gamma_0^w \quad (8)$$

where $\tau_0 = G_{12}\gamma_0$ according to the definition of G_{12} [11]; $w = 1$ for linear case; and $w \neq 1$ for nonlinear case.

It is likely that the shear stress–strain curve itself (Fig. 6a) would be close to the shear fracture stress–strain curve. Because the interface strength is variable in the discussion here, (γ_0, τ_0) can be any point on the shear fracture stress–strain curve (broken curves in Fig. 6b and c). A higher τ_0 (or higher γ_0) corresponds to a higher interface strength.

Substituting Equation 8 into Equation 6 followed by differentiation yields

$$Z = \frac{d\sigma_0^-/\sigma_0^-}{d\tau_0/\tau_0} = 1 - \frac{\lambda\gamma_0/w}{\lambda\gamma_0 + \pi f_0} \quad (9)$$

In the linear case where $w = 1$, Equation 9 coincides with Equation 7. In the nonlinear case where $w \neq 1$, it is apparent that the percentage change of the compressive strength is always less than that of the shear strength, provided that $(\lambda\tau_0/w) < (\lambda\gamma_0 + \pi f_0)$.

When $(\lambda\gamma_0/w) > (\lambda\gamma_0 + \pi f_0)$, Z would be smaller

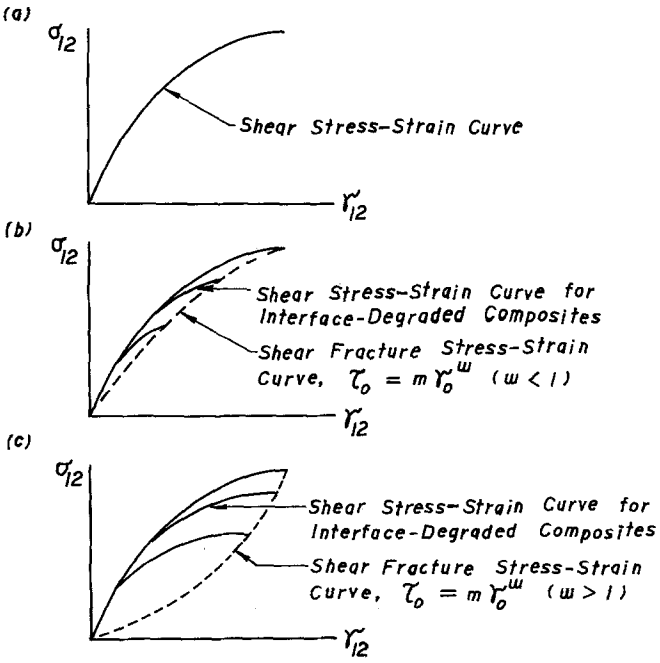

Figure 6 Shear response of composites as functions of interface conditions.

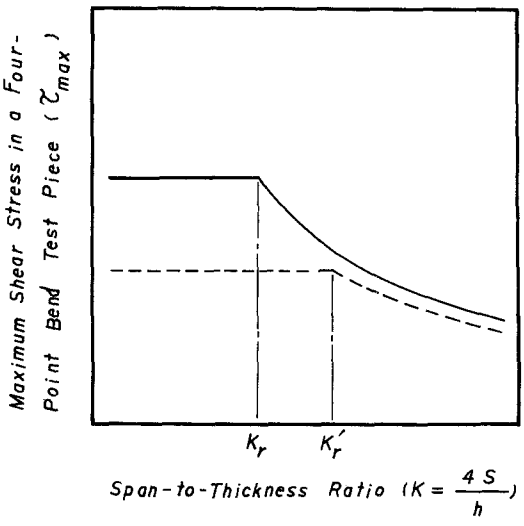

Figure 7 Failure-mode transition diagrams for unidirectional composites with different interface strengths, as derived from an extension of Wang's model [1]. (——) higher interface strength; (– – –) lower interface strength.

than zero and a decrease in shear strength may increase the compressive strength! From Inequality 5, it can be deduced that

$$\lambda\gamma_0 + \pi f_0 \geqslant 2\lambda\gamma_0 \qquad (10)$$

for most of the composites. Combining Equation 9 and Inequality 10 yields

$$Z \geqslant 1 - \frac{1}{2w}$$

Thus, to have the above mentioned unusual condition actually happen, w has to have a value between 0 and 0.5; this would not normally occur, as is apparent from the curvature of the shear fracture stress–strain curve (broken line) in Fig. 6b.

3.4. Summary

Therefore, it was proved here that generally

$$0 < Z = \frac{d\bar{\sigma}_0/\bar{\sigma}_0}{d\tau_0/\tau_0} < 1 \qquad (11)$$

Physically, it can be explained that the effect of the interface strength on the compressive strength is always less significant than that on the shear strength. This rationalization can be readily applied to construct the failure-mode transition diagram for composites with different interface conditions, as shown in Fig. 7.

4. Experimental verification

4.1. Materials preparation

Unidirectional fibreglass composites were selected for the experimental phase of this study. Type 30 pristine E-fibreglass roving was provided by Owens-Corning Fiberglas Corporation. The polymer matrix chosen is Ciba–Geigy's multifunctional epoxy resin XU235 with the aromatic diamine hardener XU205. XU235 was described as an amine-based, low viscosity resin, and recommended for "high performance filament wound structures" [15]. As suggested by the supplier, the resin was mixed with the hardener in a weight ratio of 100 : 52 prior to fabrication of the composites. In addition to the "clean" fibreglass case, two different silane coupling agents were used in the present study to vary the interface condition of unidirectional fibreglass composites:

AAPS: Dow Corning silane coupling agent Z-6020

$$(CH_3O)_3SiCH_2CH_2CH_2NHCH_2CH_2NH_2$$

AASPcS: silane coupling agent synthesized at Case [16]

$$HOSiPcOSiMe_2CH_2CH_2C_6H_4CH_2NHCH_2CH_2NH_2$$

Here, Pc designates the phthalocyninato ring system. The structural formula and other chemical details of Pc silane can be found in [3, 16].

For simplicity, composites made without coupling agents are designated as C–NoCA; those made from AAPS are designated as C–AAPS; and those made from AASPcS are designated as C′–AASPcS.

Prior to the filament winding, coating of the silane coupling agents onto the fibreglass surface was performed by dipping the pristine fibreglass into a 0.2% (by weight) aqueous solution of AAPS, or dipping into a 3.6×10^{-6} M methylene chloride solution of AASPcS, and then heating at 110° C for 30 to 45 min.

Later it was found that C′–AASPcS exhibited very poor performance. Solnik, the synthesizer of AASPcS, suggested that the heating temperature in the above described procedure might be too high to allow Pc silanes to establish stable bonding with glass surface [16]. Therefore, such a processing procedure allows the composites to possess an interface which is even more vulnerable to the moisture attack than that of C–NoCA.

4.2. Composite fabrication

The fibreglass was wound into the mould by a suitable filament winding procedure. After winding for a predetermined number of turns, the mould was assembled and ready to be impregnated by the resin. Ebert, and co-workers [4, 17, 18] had previously developed techniques for the production of nearly perfect fibreglass composites. The detailed procedure of resin infiltration by vacuum technique was the same as that which they developed previously.

After the fibreglass was impregnated by the resin, the mould assembly was cured in a water bath at 100° C for 4 h. The solidified composite is then taken out of the mould after the assembly had been cooled to room temperature. A post-curing procedure was performed in an air-circulating furnace. It consisted of heating at 150° C for 2 h; this was followed by a second heating for 2 h at 200° C.

Two different dimensions of composites were made in the present study. They were 30.5 cm × 1.27 cm × 0.190 cm and 27.9 cm × 1.27 cm × 0.432 cm. The fibre content was chosen to be about 52.5 vol %, and verified by the burn-off method [19]. Metallographic techniques were used for the quality checks; it was found that the composite made was free of major defects, that the fibre distribution was quite uniform, and that the fibre alignment was good [3].

4.3. Hydrothermal treatment and testing procedure

The mechanical properties of glass reinforced polymers decrease in the presence of moisture. The moisture-induced degradation can be accelerated by a boiling water treatment [20]. A 2 h water boil is approximately equivalent to 30 day immersion in room temperature water [21] for the material tested. Water may diffuse through the bulk resin, and along the fibre/resin interface [22, 23], thus attacking the glass surface, in both reversible and irreversible manners [24, 25]. Moisture in resins causes plasticization, swelling, and lowering of glass transition temperature [25–29]. However, the effect of water on strength of fibreglass, epoxy and polyester resin has been reported to be insignificant [30–32]. Thus, moisture-induced degradation in composites can be considered to stem mainly from interfacial degradation.

Because the epoxy resin can establish strong bonds with the glass surface even without a coupling agent [33, 34], the interface strength of glass/epoxy composites could not be varied over a wide range. Therefore, hydrothermal degradation was used in the present study to obtain various interface strengths. This methodology has been adopted by Yeung and Broutman [7, 34] to evaluate the effect of interface strength on impact performance of glass fabric composites.

To prepare test pieces for the four-point bend test, as-moulded material was cut into short pieces by a diamond wafering blade. To vary the interface conditions, some samples were subjected to boiling water immersion prior to the four-point bend test, while others were not. In the boiling water treatment, samples were placed in room temperature distilled water and heated to the boiling temperature of the water. Both ends of the sample were left bare in the water to allow moisture diffusion, and the samples were taken out of the water after the whole bath had cooled down to room temperature. These wet samples were then wiped dry and subjected to the bend test within several minutes to minimize moisture diffusion from sample surfaces.

The four-point bend tests were conducted on an Instron mechanical testing machine using a four-point bending fixture with adjustable span. In this study, two types of tests were conducted. Type 1 test was designed to allow the as-moulded (dry) test piece to fail in the flexural mode, and Type 2 test was to allow it to fail in the shear mode. The width of the test pieces was 1.27 cm. The sample thickness was 0.190 cm for Type 1 test and 0.432 cm for Type 2 test. The support span was 5.72 cm for Type 1 test and 4.80 cm for Type 2 test. The load span was 2.54 cm for both tests. The appropriate settings of the Instron machine were selected so that the loading rate was as close as possible to the ASTM standard, namely, the maximum flexural strain rate was 0.01 min^{-1} [35] in Type 1 test, and the crosshead speed was 0.127 cm min^{-1} [36] in Type 2 test (short-beam shear test).

5. Results and discussion

For Type 1 test, Equation 1 was used to calculate the apparent flexural strength for both as-moulded and moisture-degraded test pieces. The results, along with the associated failure modes, were shown in Fig. 8. It was found that C–AAPS had a very high wet strength retention even after 19 h of boiling water immersion. Because the polymer matrix of C–AAPS was open to moisture attack, it can be inferred that the flexural strength reduction of moisture-degraded C–NoCA and C′–AASPcS is caused mainly by the degradation of the interface.

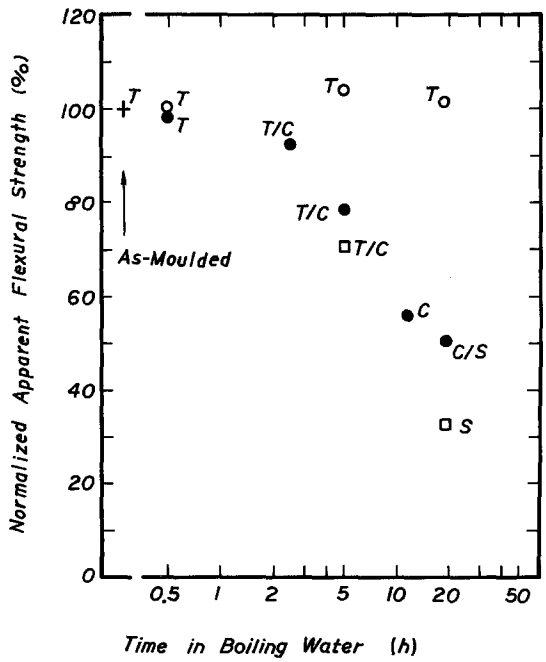

Figure 8 The effect of immersion time in boiling water on the failure modes of fibreglass composites subjected to four-point bend (flexural) tests. T: tensile failure mode; C: compressive failure mode; S: shear failure mode; T/C: tensile/compressive failure mode; and C/S: compressive/shear failure mode. (●) C–NoCA; (○) C–AAPS; (□) C′–AASPcS.

Fig. 8 also shows a series of failure mode evolution steps along with the reduction of the apparent flexural strength. Such evolution can be generalized as (flexural tensile mode) → (tensile/compressive mixed mode)→ (flexural compressive mode) → (compressive/shear mixed mode) → (shear mode). Generally speaking, the mixed mode condition does not occur at a single value of interface strength, i.e. not within a narrow range of duration of boiling water immersion. One reason for this behaviour is that the material properties show some degree of scatter. Another reason is that, in some cases, the failure event involved only one mode initially, and the second failure mode took place in the immediately following moment.

In this study, the failure mechanism in flexural compressive failure mode was that of microbuckling of fibre bundles, Fig. 9. Because the failure modes of composites showed a transition from the flexural compressive to the shear mode when the interface strength decreased, it can be concluded that Fig. 7 was conceptually correct; this in turn, verified Equation 11 experimentally.

For Type 2 test, Equation 2 was used to calculate the shear strength for both as-moulded and moisture degraded test pieces. It was found that the shear strength also decreased with increasing duration of

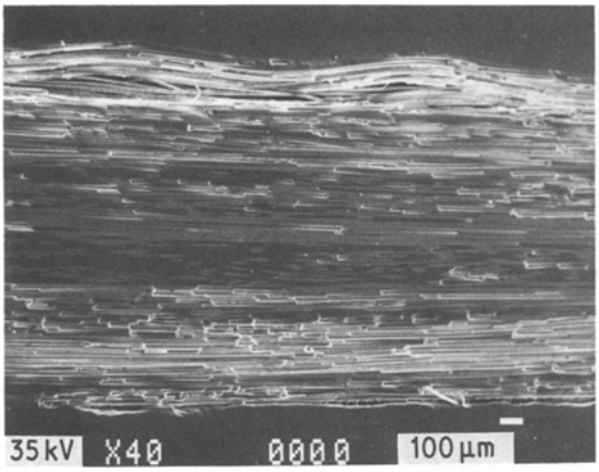

Figure 9 Scanning electron micrograph of the longitudinal section of moisture degraded fibreglass composite showing fibre microbuckling mode near the compressive side surface.

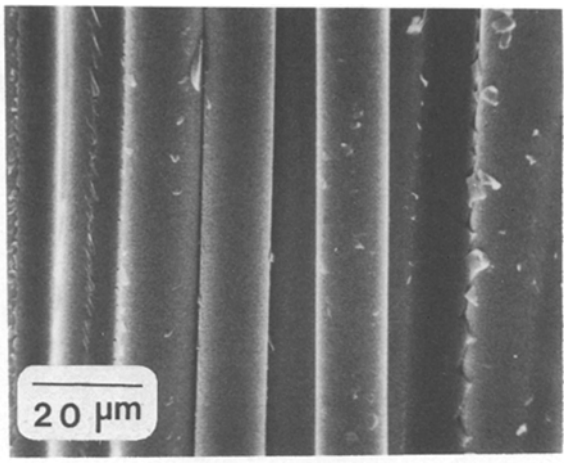

Figure 11 SEM fractograph of C′–AASPcS composite failed in static bend test. The test piece had been immersed in boiling water for 5 h prior to the bend test.

boiling water immersion [3], and that the shear failure mode remained the same throughout the test. The fact that no failure mode transition occurred also supported the correctness of Fig. 7.

Fractographic study on the broken test pieces showed that, shear cracks extended mainly along the fibre/matrix interface. This indicated that the fibre/matrix interface was the weakest portion of the composites tested. There were many tiny, residual matrix particles adhered on the fibre surfaces of all as-moulded (dry) test pieces, Fig. 10. This feature was found regardless of the coupling agents used. For moisture degraded test pieces, C′–AASPcS and C–NoCA showed relatively clean fibre surface and debonded fibre/matrix interfaces, Figs 11 and 12. On the other hand, hydrothermal treated C–AAPS exhibited closely spaced hackle patterns in the epoxy matrix which adhered rigidly to the fibre surface, Fig. 13. Therefore, the fractography was closely related to the trend in the apparent flexural strength (Fig. 8), and the assumption of this test, the fact that the moisture-induced degradation in fibreglass composites was caused mainly by interfacial degradation, was satisfactorily justified.

The experimental phase which serves to verify the theoretical prediction has certain shortcomings. Firstly, the moisture content in the mid-thickness layer and in the outermost layer may be different because of the finite moisture diffusion rate for a test piece subjected to a particular duration of boiling water immersion treatment. This implies that the interface condition near the surface of the test piece may be poorer than that in the mid-thickness layer. Because the flexural strength is affected by the interface condition near the surface and the shear strength is affected by that in the centre of the test piece, the two flexural/shear mechanisms really competed with each other on a slightly different interface scale for the bend test of any moisture-degraded test piece. Secondly, so far as the moisture diffusion rate is concerned, because the Type 2 test piece is thicker than the Type 1 test piece, the moisture-degraded shear strength of the former would always be higher than that of the latter. Additionally, the differences in specimen size and strain rate between Type 1 and Type 2 tests also play a minor role in causing the difference in moisture-degraded shear strengths. Therefore, no quantitative attempt was made here to construct a

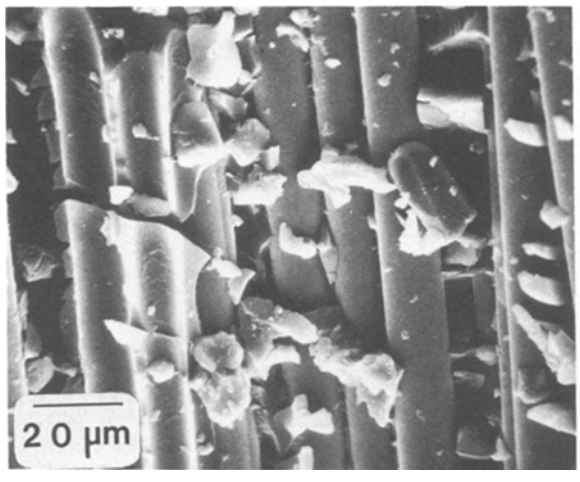

Figure 10 SEM fractograph of as-moulded C′–AASPcS composite failed in static bend test.

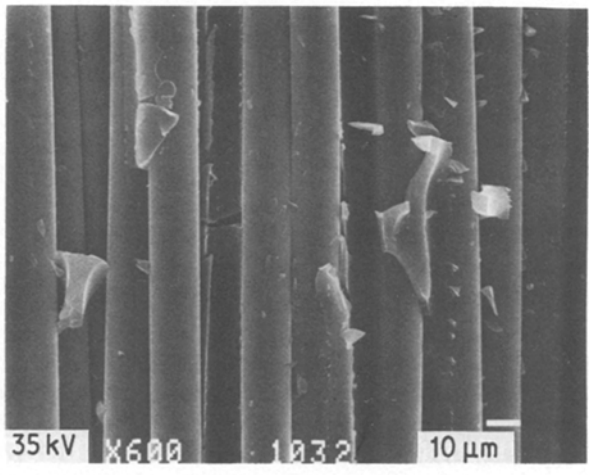

Figure 12 SEM fractograph of C–NoCA composite failed in static bend test. The test piece had been immersed in boiling water for 5 h prior to the bend test.

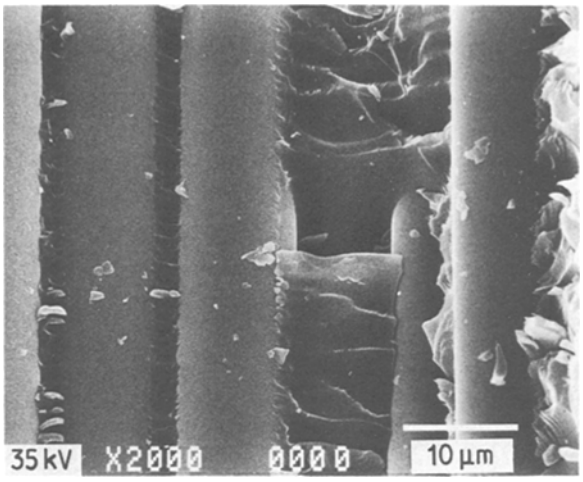

Figure 13 SEM fractograph of C–AAPS composite failed in static bend test. The test piece had been immersed in boiling water for 5 h prior to the bend test.

"real" failure-mode transition diagram such as that shown schematically in Fig. 7.

6. Conclusions

When the fibre/matrix interface changed, both the compressive and the shear strengths of composites were affected in the same sense as the interface strength. The relative change of the compressive strength is always smaller than that of the shear strength. As a consequence, a four-point bending test piece which normally fails in the flexural compressive mode may fail in the shear mode when the interface strength decreased. Such a phenomenon was verified both theoretically and experimentally, and was demonstrated in both Equation 11 and Fig. 7.

Based on the above argument, a bend test piece which normally failed in the shear mode may fail in the flexural compressive mode when the interface strength increased. Also, because the purpose of the hydrothermal treatment was one of degrading the interface of the fibreglass composites, the above rationalization is not restricted to the moisture-degraded composites only. It should be valid for any other "dry" composites with different fibre surface treatment. Therefore, such an understanding not only serves as a guide for designing a valid bend test for which the failure mode is predictable, but also serves as a rule-of-thumb for estimating the interface conditions of any new system of composites.

Acknowledgements

The authors are pleased to acknowledge the support of this research by the Materials Research Laboratory of Case Western Reserve University and the National Science Foundation under Grant No. DMR80-20245. The authors are also grateful to Dr J. S. Jen of Owens-Corning Fiberglas Corporation for supplying the Type 30 pristine E-fibreglass roving, and to the staff of Delsen Testing Laboratories, Inc. for their help in preparing the manuscript.

References

1. A. S. D. WANG, ASME Paper No. 78-WA/Aero-1 (1978).
2. C. E. BROWNING, F. L. ABRAMS and J. M. WHITNEY, in ASTM STP 797 (1983) p. 54.
3. C. SHIH, PhD thesis, Case Western Reserve University, Cleveland, Ohio (1985).
4. H. C. KIM, PhD thesis, Case Western Reserve University, Cleveland, Ohio (1978).
5. M. H. TELICH, MS thesis, Case Western Reserve University, Cleveland, Ohio (1980).
6. M. DAVIDOVITZ, A. MITTELMAN, I. ROMAN and G. MAROM, *J. Mater. Sci.* **19** (1984) 377.
7. P. YEUNG and L. J. BROUTMAN, in SPI RP/C 32nd Annual Technical Conference (The Society of the Plastics Industry, New York, 1977) Section 9-B.
8. N. L. HANCOX, *J. Mater. Sci.* **7** (1972) 1030.
9. L. G. BEVAN, *Composites* **8** (1977) 227.
10. L. B. GRESZEZUK, "Microbuckling of Unidirectional Composites", AFML-TR-71-231.
11. S. W. TSAI and H. T. HAHN, in "Introduction to Composite Materials" (Technomic Publishing, Westport, CT, 1980) pp. 416–18.
12. J. G. DAVIS, "Compressive Strength of Fibre-reinforced Composite Materials", in ASTM STP 580 (American Society for Testing and Materials, Philadelphia, Pennsylvania, 1975) p. 364.
13. D. L. HARROD and R. T. BEGLEY, in SAMPE, Vol. 10 (Society of Aerospace Material and Process Engineers, CA, 1966) p. E-1.
14. J. G. DAVIS, "Compressive Instability and Strength of Uniaxial Filament-reinforced Epoxy Tubes", NASA-TN-D569 (1970).
15. Catalog and technical information on XU235 and XU205 (Ciba-Geigy Corporation, Ardsley, NY, 1982).
16. D. F. SOLNIK, PhD thesis, Case Western Reserve University, Cleveland, Ohio (1985).
17. H. C. KIM and L. J. EBERT, *J. Compos. Mater.* **12** (1978) 139.
18. A. K. JAIN, MS thesis, Case Western Reserve University, Cleveland, Ohio (1981).
19. ASTM D 2584-68, "Standard Test Methods for Ignition Loss of Cured Reinforced Resins".
20. T. C. KOSKY, D. K. BANERJEE and P. N. GOVINDARAJAN, in SPI RP/C 29th Annual Technical Conference (The Society of the Plastics Industry, Inc., New York, 1974) Section 2-B.
21. E. P. PLUEDDEMANN, in "Silane Coupling Agents" (Plenum Press, New York, 1982) p. 14.
22. W. D. McNEIL, B. BENNETT and R. I. LEININGER, in SPI RP 19th Annual Technical and Management Conference (The Society of the Plastics Industry, New York, 1964) Section 11-B.
23. J. DELMONTE and E. BARNA, in SPI RP 18th Annual Technical and Management Conference (The Society of the Plastics Industry, New York, 1963) Section 20-A.
24. M. K. ANTOON, PhD thesis, Case Western Reserve University, Cleveland, Ohio (1980).
25. R. E. TRABOCCO and M. STANDER, in ASTM STP 602 (American Society for Testing and Materials, Philadelphia, Pennsylvania, 1975).
26. C. E. BROWNING and J. M. WHITNEY, in "Fillers and Reinforcements for Plastics", edited by R. D. Deanin and N. R. Schott (Adv. Chem. Ser. No. 134, ACS, Washington, DC, 1974) Ch. 14.
27. R. DEIASI and J. B. WHITESIDE, in ASTM STP 658 (1978) p. 2.
28. C. E. BROWNING, in SPI RP/C 28th Annual Technical Conference (The Society of the Plastics Industry, New York, 1973) Section 15-A.
29. C. E. BROWNING and J. T. HARTNESS, in ASTM STP 546 (1975) p. 284.
30. D. A. SCOLA, in SPI RP/C 30th Annual Technical Conference (The Society of the Plastics Industry, New York, 1975) Section 22-C.
31. T. SUZUKI, *Reinforced Plastics* (*Jpn.*) **18** (1972) 331.
32. K. ENDO and S. ISHIHARA, *J. Soc. Mater. Sci.* (*Jpn.*) **15** (1966) 561.

33. B. D. AGARWAL and L. J. BROUTMAN, in "Analysis and Performance of Fiber Composites" (Wiley, New York, 1980).
34. P. YEUNG and L. J. BROUTMAN, *Polym. Eng. Sci.* **18** (1978) 62.
35. ASTM D 790-84, "Standard Test Methods for Flexural Properties of Unreinforced and Reinforced Plastics and Electrical Insulating Materials" (American Society for Testing and Materials, Philadelphia, Pennsylvania, 1984).
36. ASTM D 2344-76, "Standard Test Method for Apparent Interlaminar Shear Strength of Parallel Fiber Composites by Short-Beam Method" (American Society for Testing and Materials, Philadelphia, Pennsylvania, 1984).

Received 25 October 1985
and accepted 21 January 1986